

STED microscopy: make the invisible visible

Julia Neuwirth

July to September 2015

Abstract

Modern microscopes allow us to image intracellular structures with a resolution of ~ 250 nm. Novel nanoscopy techniques push the imaging resolution even further, down to the tens of nanometer scale (~ 25 nm). With fluorescence labeling, we can distinguish different populations of proteins and observe their interactions. Typically, we distinguish fluorophores based on their emission spectrum.

One type of nanoscopy, STimulated Emission Depletion (STED) nanoscopy, relies on a high-powered "depletion laser" at the far-red end of the emission spectrum. To reduce cost and circumvent bleaching issues, it is advantageous to implement only a single depletion laser. This, however, requires that the imaged fluorophores have overlapping emission spectra, which, in turn, makes it difficult to distinguish more than two fluorophores.

It has been shown that it is possible to distinguish fluorophores based on their fluorescence lifetime using linear unmixing. Motivated by the potential to use this method for imaging more than two fluorophores, I present a simulation-based study, in which I use linear unmixing to separate two fluorescent dyes (SiR and ATTO590) based on their fluorescence lifetime. I show that relatively high photon counts are needed to reliably distinguish the two dyes, likely making the lifetime-based unmixing an insufficient means to distinguish dyes in live-cell STED images where photon counts are very low.

Another challenge associated with STED nanoscopy is photobleaching. It is

established that different scanning parameters (e.g. scan speed) and buffer solutions affect the rate of photobleaching in fluorescence microscopy, however, these variables have not been tested systematically on our custom-built STED nanoscope. Here I present a preliminary study on the dependence between photobleaching of the popular SiR-647 dye and the factors imaging speed and buffer solutions.

I conducted the work presented here during my stay at the Bewersdorf Laboratory at the Department of Cell Biology, Yale University School of Medicine.

Contents

1	Introduction	4
1.1	Fluorescence, STED and photobleaching	4
1.2	STED nanoscopy	6
1.3	Fluorophores	8
1.3.1	ATTO590	8
1.3.2	SiR-647	8
2	Multi-color STED	10
2.1	Unmixing	11
2.1.1	Simulation	11
2.1.2	Testing of lifetimes	13
3	Photobleaching	22
3.1	Bleaching and the field of view size	22
3.2	Photobleaching and oxygen scavenging buffers	24
3.3	Conclusion on bleaching experiments	
	26	
A	Matlabcode	27
B	Sample preparation	37
B.1	Fixed cell	37
B.2	Live cell	37
B.3	Oxygen scavenging buffers	37
B.3.1	dStorm buffer	37
B.3.2	OxyFluor	37
C	Bleaching analysis	38
C.1	Oxygen scavenging buffers	38
C.2	Field of view	38

1 Introduction

Fluorescence microscopy is one of the most widely used techniques for investigating biological processes at the cellular and sub-cellular level. One major advantage of fluorescence microscopy is the possibility to detect specific cellular components through fluorescence labeling. Another advantage is that fluorescence microscopy allows to observe structures inside a living sample in real time. Due to the diffraction of light, the resolution of conventional fluorescence microscopes is limited to 200-300 nm in the lateral direction and 500-700 nm axially. Novel nanoscopy (or "super-resolution fluorescence microscopy") techniques circumvent this so-called diffraction limit, i.e. STimulated Emission Depletion (STED), REversible Saturable Optically Linear Fluorescence Transition (RESOLFT) and STochastic Optical Reconstruction Microscopy (STORM) nanoscopy, which is also known as Fluorescence Photoactivation Localization (FPALM/PALM) Microscopy.¹

1.1 Fluorescence, STED and photobleaching

Fluorescence is a spontaneous emission of light by a material after excitation with an external source. A fluorescence microscope forms an image based on fluorescence detected from fluorescent molecules (also called fluorophores) attached to structures of interest.²

Fluorescence is rooted in transitions between energy states of a fluorophore. When a fluorophore absorbs a photon in the appropriate wavelength range, its electron configuration changes to a state of higher energy, the excited state.³ This higher energy state is unstable. Hence, after a few nanoseconds (fluorescence lifetime), the

¹GouldTJ et al., "Optical nanoscopy: from acquisition to analysis", *Annu Rev Biomed Eng.* 2012;14:231-54. doi: 10.1146/annurev-bioeng-071811-150025. Epub 2012 May 3.

²Lakowicz Joseph R.: *Principles of Fluorescence Spectroscopy*, Springer 2006
ISBN: 9780387463124 9780387312781

³Franisco M. Raymo, "Photoactivatable Fluorophores," *ISRN Physical Chemistry*, vol. 2012, Article ID 619251, 15 pages, 2012. doi:10.5402/2012/619251

molecule falls back the ground state by releasing energy in the form of a photon (i.e. light).⁴ The Jablonski diagram illustrates these transitions between different energy levels (see Fig. 1). Each line of the diagram represents a different energy level, or state, of the fluorophore. In STED nanoscopy the depletion laser forces specific excited fluorophores to the ground state through release of a photon with a wavelength matching the wavelength of the depletion laser (see Fig. 2).

When a fluorophore is in the excited state, there is also a (low) probability that it will transition into the so-called "triplet state". If a fluorophore gets to the triplet state, it stays there for a relatively long time before returning to the ground state, for example through a process called phosphorescence; a specific type of photoluminescence related to fluorescence. Phosphorescence lifetimes are up to milliseconds or seconds.⁵ When in an excited state (singlet or long-lived triplet), the fluorophore is more likely to undergo chemical interactions with neighboring molecules (maybe oxygen molecules). This may result in the formation or breaking of covalent bonds in the fluorophore, disrupting its ability to fluoresce; a process called photobleaching.

⁴T-Pengo, "Spectral unmixing of multiply stained fluorescence samples", *Microscopy: Science, Technology, Applications and Education* A. Mendez-Vilas and J. Diaz (Eds.), Formatex 2010

⁵M.G. Neumann, C.C. Schmitt, et al., "The initial radical yields and the efficiency of polymerisation for various dental photo initiators excited by different light curing units", *Dental Materials* 22, pp. 576-584, 2006

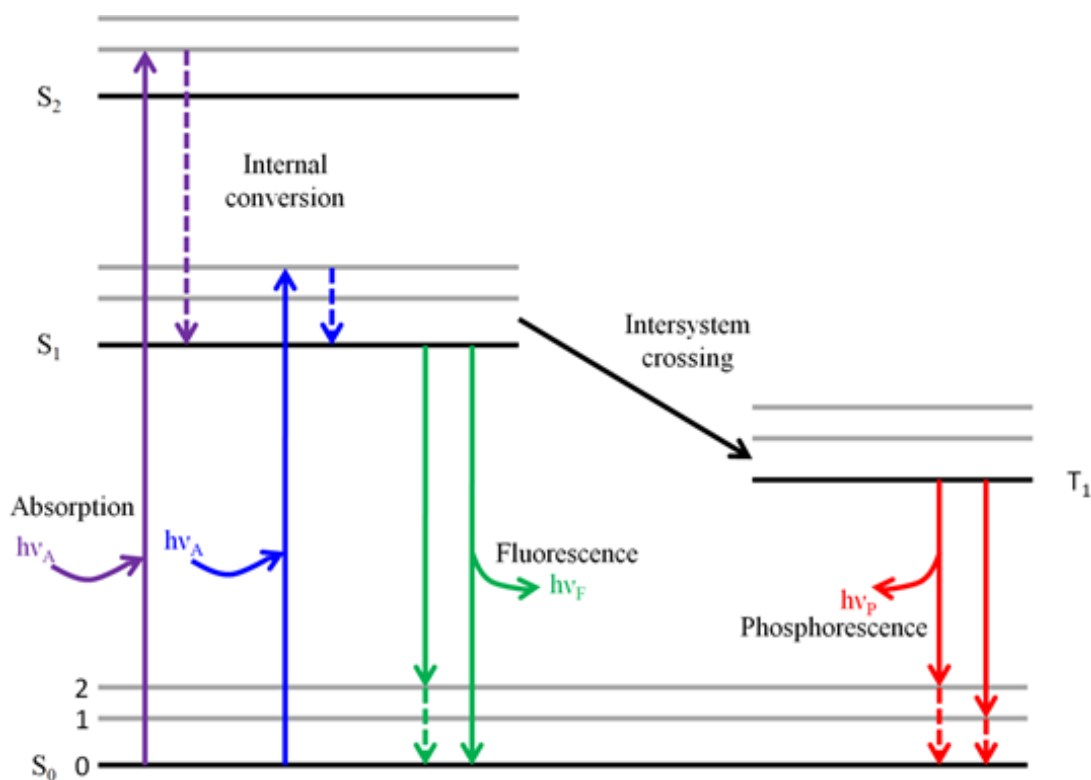


Figure 1: Jablonski Diagram

1.2 STED nanoscopy

STED nanoscopy is a powerful fluorescence imaging technique, which overcomes the resolution limit of conventional microscopy using a purely physics-based "trick". In STED nanoscopy, resolution below the diffraction limit is achieved by introducing a so-called depletion laser, which depletes the excited state of a fluorophore, forcing it to release its energy in the form of a far-red shifted photon, which is filtered out from the normal spontaneously emitted fluorescence-photons. Importantly, the wavefront of the depletion beam is modified such that it forms a ring-shaped focus in the sample plane. This depletion focus is aligned with the excitation focus to inhibit fluorescence at the periphery of the excitation focus, thereby ensuring that all detected photons originate from the very center of the excitation focus, where the

depletion laser intensity is zero (see Fig. 2).

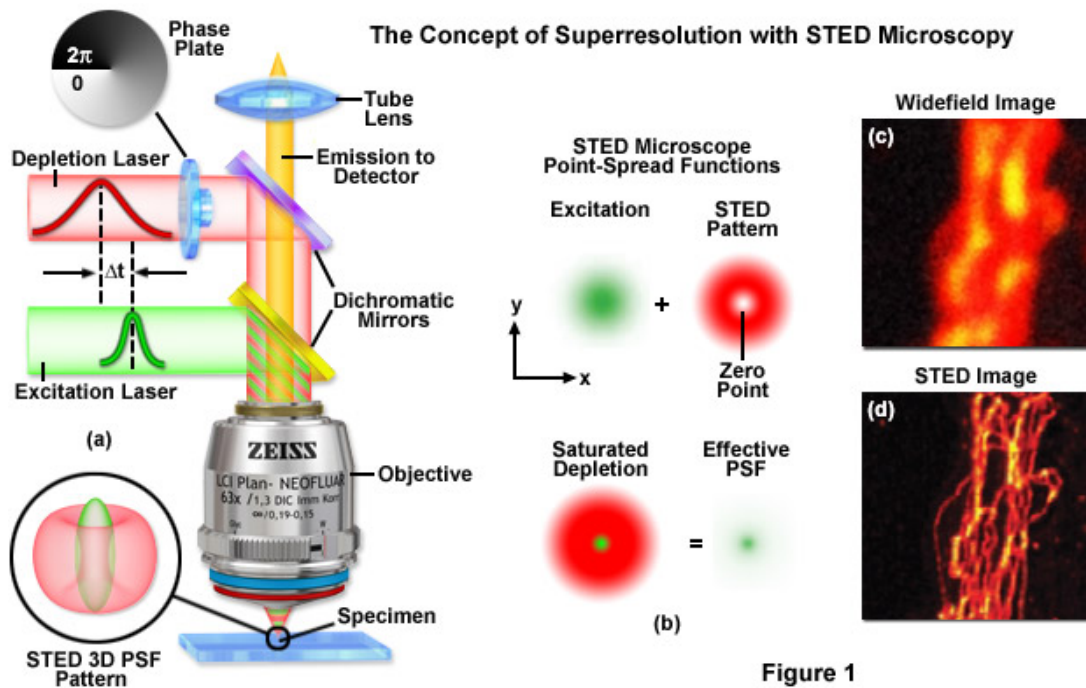


Figure 1

Figure 2: Concept of STED nanoscopy.

Two different lasers are used in STED nanoscopy: The excitation laser (green) is used to excite fluorophores, whereas the depletion laser (red) forces the excited fluorophores back to the ground state by emitting photons at the wavelength of the depletion laser. The wavefront of the depletion laser beam is modified by a phase plate (typically a "vortex" or "top-hat" phase plate), giving rise to a ring-shaped laser focus. Fluorophores are only allowed to relax to the ground state via spontaneous fluorescence in the middle of the ring where the intensity of the depletion laser is zero.⁶

Challenges in STED nanoscopy

STED nanoscopy is associated with a relatively high degree of photobleaching.⁷ This bleaching becomes particularly problematic, when studying live-cell dynamics,

⁶Zeiss: "STED Microscopy"
<http://zeiss-campus.magnet.fsu.edu/tutorials/superresolution/stedconcept/indexflash.htm>
 (15.8.2015)

⁷S. W. Hell, "Nanoskopie mit fokussiertem Licht", www.prophysik.de/details/articlePdf/1104523/issue.html

which requires continuous acquisition of images in the same field of view (FOV). If bleaching is too severe the last images of the sequence will be completely dark due to a lack of signal. Therefore, to improve image quality for STED nanoscopy, it is essential to account for photobleaching.

1.3 Fluorophores

In this study, I used two different organic dyes: ATTO590 and SiR-647. Both dyes are popular labels for STED nanoscopy with a depletion wavelength at ~ 775 nm.

1.3.1 ATTO590

ATTO590 is a fluorescent dye belonging to the class of rhodamine dyes. The absorption maximum is at 594 nm and the emission maximum is at 624 nm. It is membrane permeable, hence it is useful for labeling intracellular structures in living cells. The chemical structure is shown in the figure below.⁸

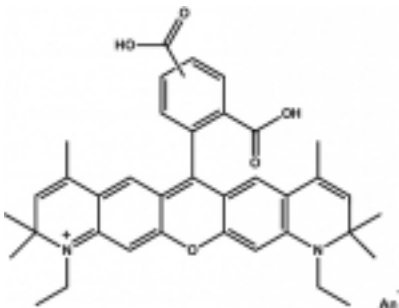


Figure 3: Structure of ATTO590.

1.3.2 SiR-647

The silicon rhodamine dye, SiR-647, is spectrally similar to ATTO647N with an absorption maximum at 645 nm and emission maximum at 661 nm. Like ATTO590,

⁸ATTO-Tec: "ATTO590", <https://www.atto-tec.com> (08.15.2015)

it is membrane permeable. The chemical structure is shown in the figure below.

9

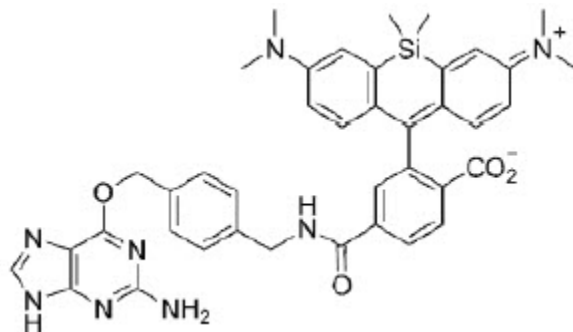


Figure 4: Structure of SiR-647.

A SNAP-tag for binding to the SNAP fusion protein (for example, inside living cells) is shown on the left hand side, whereas the molecular structure of the SiR-647 dye is on the right hand side.

⁹Bio Labs: "SNAP-Cell 647-SiR", <https://www.neb.com/products/s9102-snap-cell-647-sir> (20.8.2015)

2 Multi-color STED

Multi-color fluorescence imaging typically exploits the spectral diversity between fluorophores to visualize differently labeled structures (see Fig. 5). To image more fluorophores, more detection channels are required. One inherent challenge of multi-color fluorescence imaging is the relatively broad emission spectrum of most fluorophores, which often makes the fluorescence signal from one fluorophore "bleed through" to a detection channel (spectral band) not dedicated to that fluorophore; this phenomenon is called "cross-talk". If cross-talk is not accounted for, fluorophore identification becomes ambiguous. Fortunately, cross-talk can often be compensated for with the widely used post-processing method called spectral unmixing

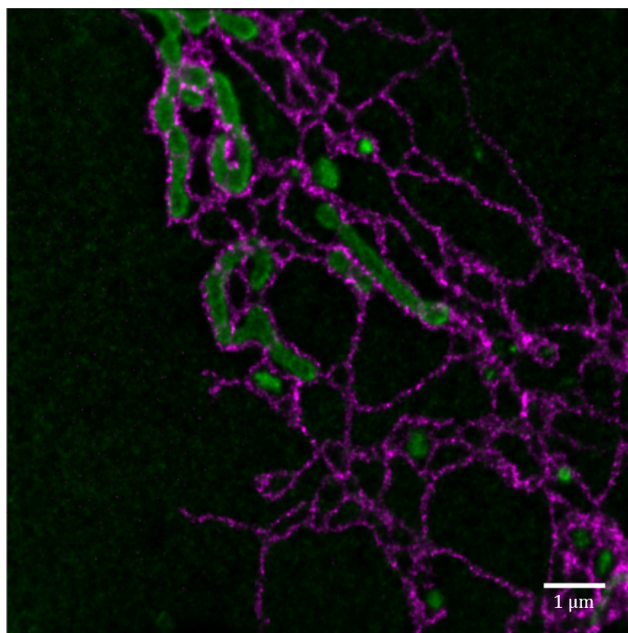


Figure 5: Example of two-color STED nanoscopy.

The first frame of a live-cell STED image of interacting mitochondria and endoplasmic reticulum (ER). The ER is labeled with Halo-Sec61 β with SiR-CA (magenta) and the mitochondria with a SNAP-OMP25 with 590-BG (green). This image was acquired with two relatively narrow fluorescence detection bands, one for each fluorophore. Therefore, unmixing was not required to distinguish the two dyes. On the downside, much signal from each fluorophore fell outside the dedicated detection bands, resulting in a dimmer signal than could be obtained with broader detection bands.¹⁰

2.1 Unmixing

If two fluorophores have overlapping spectra, it is difficult to acquire the signal from one fluorophore without also detecting some signal from the other. Spectral unmixing is a data processing technique, which uses the known fluorescence spectra to recover the distribution of each fluorophore based on the mixed signals from different detectors. While spectral unmixing is a more commonly used technique, it is also possible to differentiate fluorophores based on differences between their fluorescence lifetimes.¹¹

Here, I applied the linear unmixing approach typically used for spectral unmixing, in an attempt to separate two fluorophores based on their lifetimes; an approach which would be very useful when the emission spectra of the used dyes are very similar. First, I made a simulation to assess whether linear unmixing based on fluorescence lifetime works with the lifetimes measured on our custom built STED nanoscope.

2.1.1 Simulation

In my simulation I focused on the two described dyes, ATTO590 and SiR-647. I used empirically measured lifetimes and varied the number of photons detected from each dye between 25 and 1000. I wrote the simulation program, described below, in MATLAB (MathWorks) (see Appendix A).

The program simulates two time-gated detection channels, with an adjustable time-gap between them. Based on the known (measured) lifetimes of two fluorophores, the program computes a linear unmixing matrix between the two detection channels (see below). Again, based on the known lifetimes, but also based on the specified photon counts, the program then simulates the photon counts in each detection channel with Poisson-distributed shot-noise in each detection channel. The program then

¹⁰Bottanelli et al. (nature communications, in press)

¹¹Johanna Bueckers, Dominik Wildanger, Giuseppe Vicidomini, Lars Kastrop, Stefan W. Hell, "Simultaneous multi-lifetime multi-color STED imaging for colocalization analyses," *Opt. Express* 19, 3130-3143 (2011); <https://www.osapublishing.org/oe/abstract.cfm?URI=oe-19-4-3130>

unmixes the simulated data, estimating the number of photons detected from each dye. This simulation is executed multiple times (with different seeds for the shot-noise generator), to also provide a standard deviation of the estimate. This process is executed for different widths of the time-gap between the two detection channels (see Fig. 6). When one of the detection windows gets too small (time width = 0 ns), the center position of the time-gap is shifted by 1 ns and the time-gap between the two detection windows is reset to zero. The program runs this scheme until all possible widths and center positions of the time-gap are simulated. The results of the simulation with different fluorescence lifetimes and different photon counts are shown below.

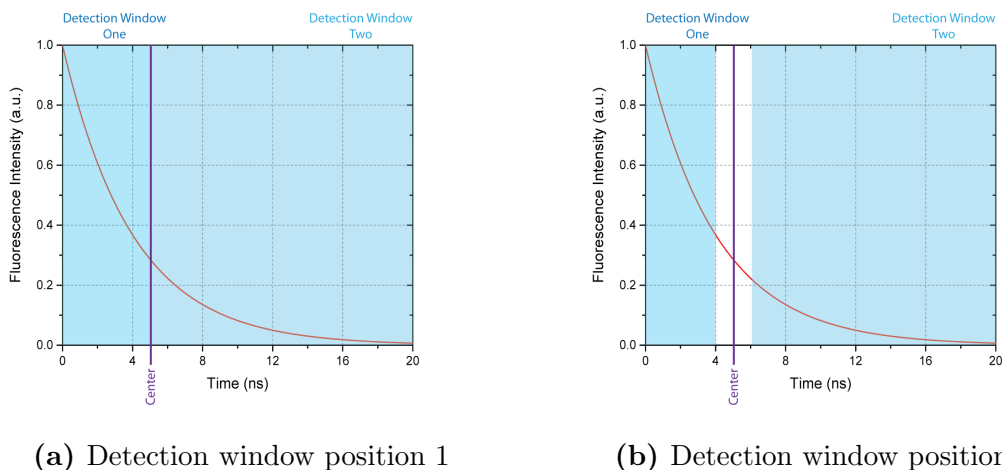


Figure 6: Simulated detection channels.

The detection windows start at a given position and get smaller after each iteration (as the width of the time-gap increases). Photons emitted during the time-gap (blank area between the detection windows) are not detected. This iteration proceeds until the width of one detection window reaches zero.

The linear unmixing matrix consist of four entries, calculated below.

$$a_{11} = \frac{1}{\int_0^{inf} e^{-\frac{t}{\tau_{One}}} dt} \int_{startWindowOne}^{endWindowOne} e^{-\frac{t}{\tau_{One}}} dt$$

$$a_{12} = \frac{1}{\int_0^{inf} e^{-\frac{t}{\tau_{Two}}} dt} \int_{startWindowOne}^{endWindowOne} e^{-\frac{t}{\tau_{Two}}} dt$$

$$a_{21} = \frac{1}{\int_0^{inf} e^{-\frac{t}{\tau_{One}}} dt} \int_{startWindowTwo}^{endWindowTwo} e^{-\frac{t}{\tau_{One}}} dt$$

$$a_{22} = \frac{1}{\int_0^{inf} e^{-\frac{t}{\tau_{Two}}} dt} \int_{startWindowTwo}^{endWindowTwo} e^{-\frac{t}{\tau_{Two}}} dt$$

These entries are used for linear unmixing, i.e. solving the equation below:

$$\begin{pmatrix} WindowOnePhotons \\ WindowTwoPhotons \end{pmatrix} = \begin{bmatrix} a_{11} & a_{12} \\ a_{21} & a_{22} \end{bmatrix} \begin{pmatrix} Photons\ from\ dye\ 1 \\ Photons\ from\ dye\ 2 \end{pmatrix}$$

By solving this linear equation, the photon counts from the first and the second dye will be calculated. The two resulting photon counts are combined into a ratio (i.e. one estimated photon count divided by the other). The mean value of this ratio and its standard deviation gets stored for each simulated detecting setting (time-gap width and time-gap center position). For a more detailed explanation, please refer to the attached code in the appendix.

2.1.2 Testing of lifetimes

I used my program to test several different parameters. First, I simulated two hypothetical dyes with well separated lifetimes of 4 ns (lifeTimeONE¹²) and 2 ns (lifeTimeTWO¹³). Next, I simulated data based on empirically measured lifetimes of the two discussed STED-compatible dyes, ATTO590 and SiR-647. The lifetime of ATTO590 was 4.08 ns (implemented as lifeTimeONE) and the lifetime of SiR-647 was 3.37 ns (implemented as lifeTimeTWO). These lifetimes were measured in fixed COS7 cells (either immunostained with ATTO590 or labeled with SiR-647 via SNAP-tag) using a custom-built STED nanoscope with adjustable temporal detection windows.

¹²lifetime of the first dye

¹³lifetime of the second dye

Not only the fluorescence lifetimes were changed in the program, I also varied the number of detected photons from the two dyes (implemented as photonsONE and photonsTWO). The known (true) ratio between photonsONE and photonsTWO should be compared to the ratio estimated in the simulation. I tried three different settings: For **(a)**, I used a "low" number of 25 photons for photonsONE and 50 photons for photonsTWO, for **(b)** I used a "medium" number of 400 photons for photonsONE and 200 photons for photonsTWO, and for **(c)** I used a "high" number of 1000 photons for photonsONE and 500 photons for photonsTWO. According to the simulated number of photons the resulting ratios of the dye concentrations should be 2 for every setting.

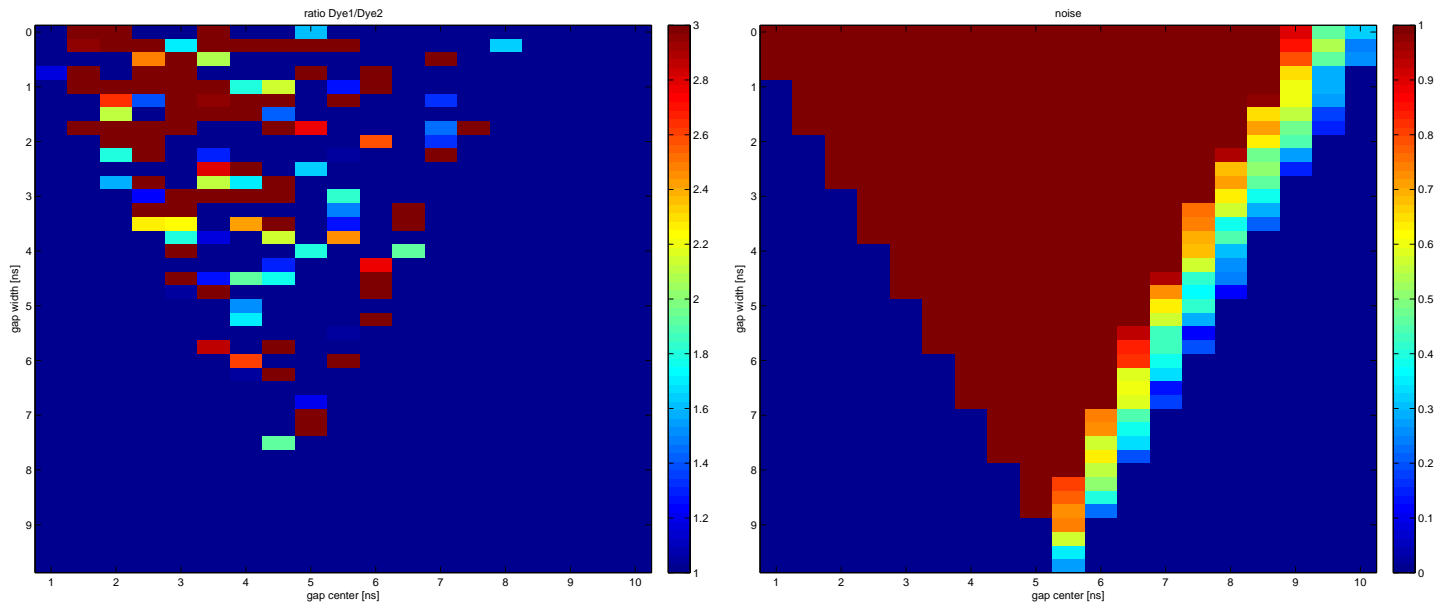
Figures below (7- 12) show the time-gap center position on the abscissa and the width of the time-gap between the two detection channels on the ordinate. Pixel colors represents the estimated ratio between photon counts from the two dyes (left) and the corresponding standard deviation of the estimate (right). Ideally, my program should return a ratio with a value of 2 (light green) and a standard deviation of 0 (dark blue).

a) Low Signal

In this simulation the number of photons per dye was set to 50 for photonsONE and 25 for photonsTWO.

a.1) Hypothetical dyes with well separated lifetimes.

LifeTimeONE = 4 ns, LifeTimeTWO = 2 ns.



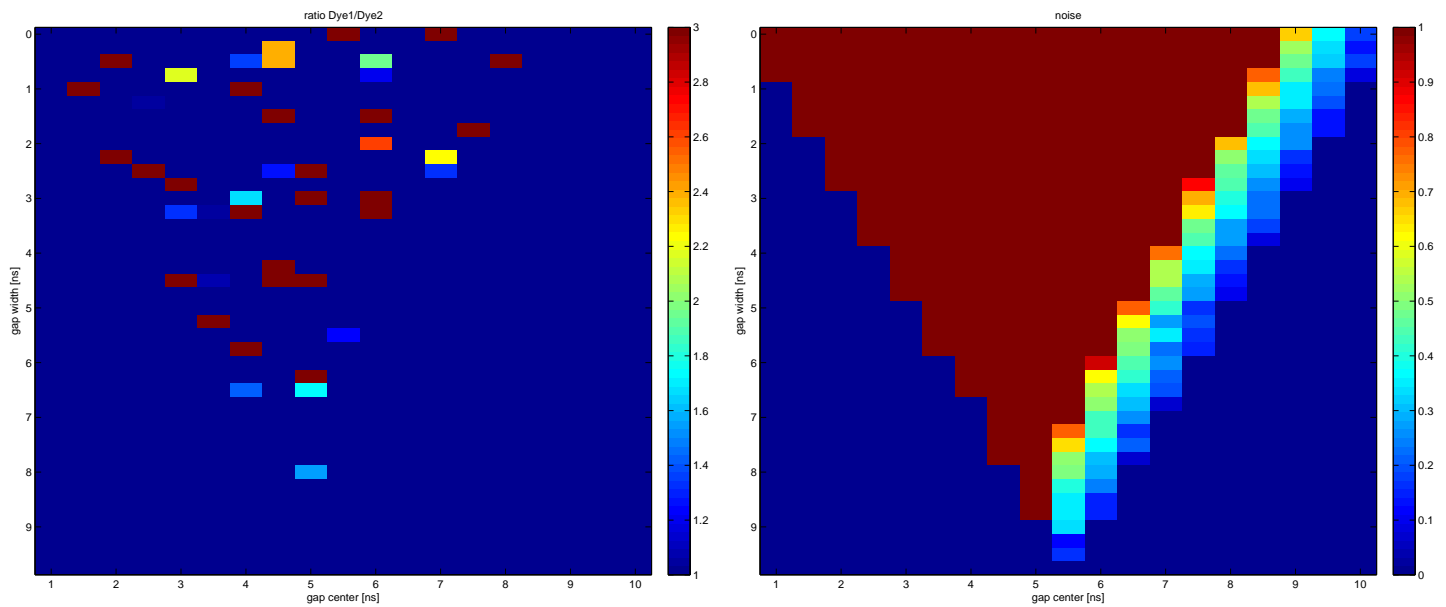
(a) Ratio of Dye1/Dye2

(b) Noise

Figure 7: Hypothetical dyes with lifetimes of 4 ns and 2 ns and photon counts of 50 and 25.

In this simulation, a ratio of 2 was not reliably achieved. Due to the simulated shot-noise, the standard deviation of the estimated ratio is always higher than 1, corresponding to more than 50 % of the resulting signal. Hence, the program could not separate the two dyes with the given photon counts and settings for fluorescence lifetime.

a.2) Lifetime of ATTO590 and SiR-647



(a) Ratio of Dye1/Dye2

(b) Noise

Figure 8: Unmixing of ATTO590 and SiR with lifetimes of 4.08 ns and 3.37 ns and photon counts of 50 and 25.

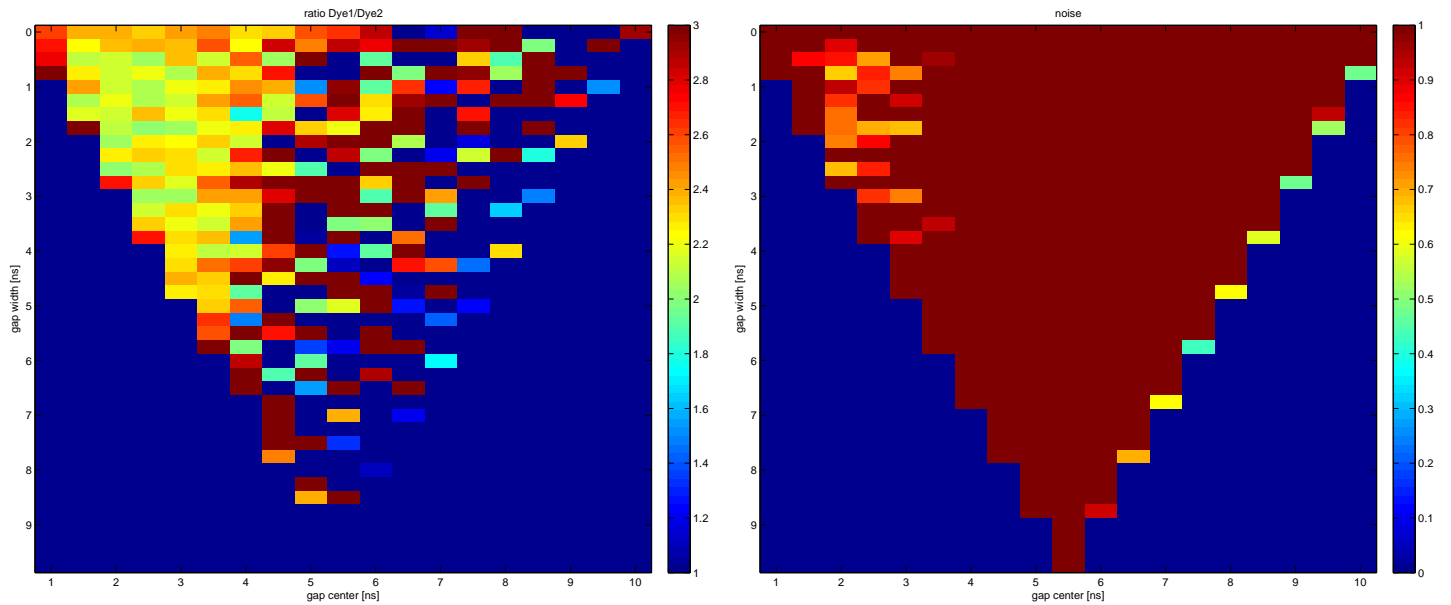
Also in this simulation, a value of 2 was not reliably achieved.

b) Average Signal

In this simulation the number of photons per dye was set to 400 for photonsONE and 200 for photonsTWO.

b.1) Hypothetical dyes with well separated lifetimes.

LifeTimeONE = 4 ns, LifeTimeTWO = 2 ns.



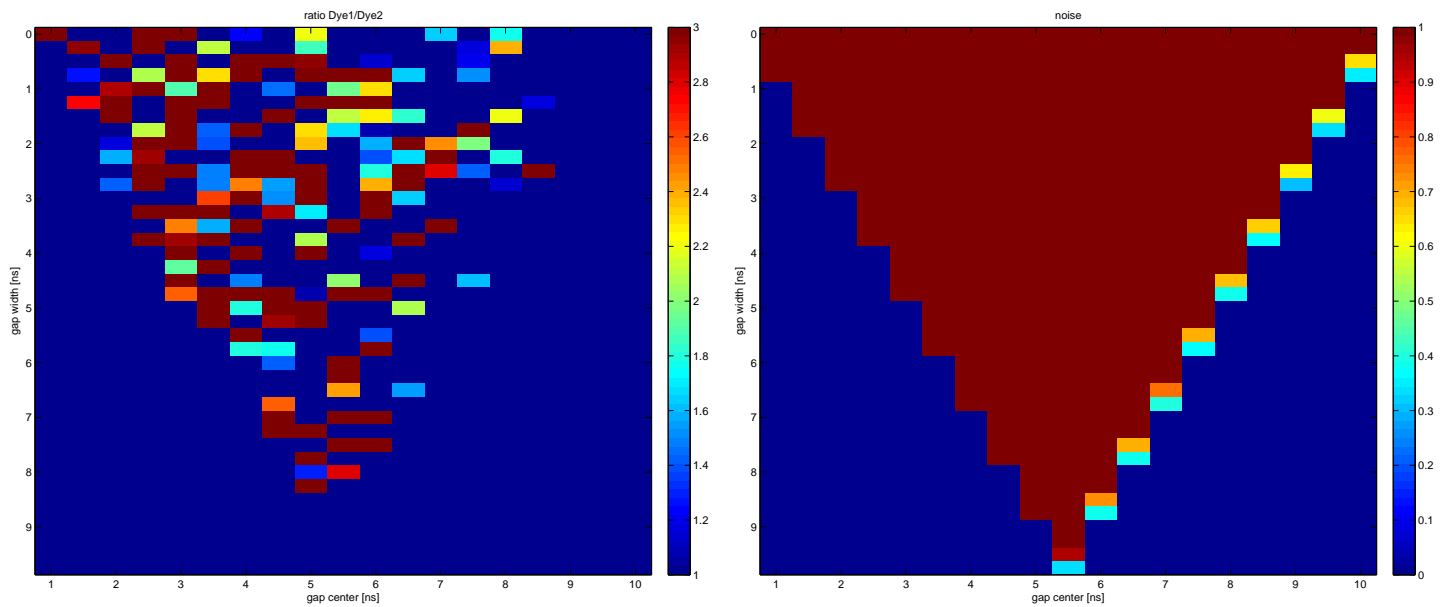
(a) Ratio of Dye1/Dye2

(b) Noise

Figure 9: Hypothetical dyes with lifetimes of 4 ns and 2 ns and photon counts of 400 and 200.

When the photon count increases, the photon-ratio-estimate improves significantly (see values near 2 in the upper left corner [relatively small width of the time-gap and time-gap centering around 2 ns]). This might allow a separation of dyes with a lifetime of 4 ns and 2 ns. However, the standard deviation of the estimate is about 0.7, corresponding to an error of more than 36 %.

b.2) Lifetime of ATTO590 and SiR-647



(a) Ratio of Dye1/Dye2

(b) Noise

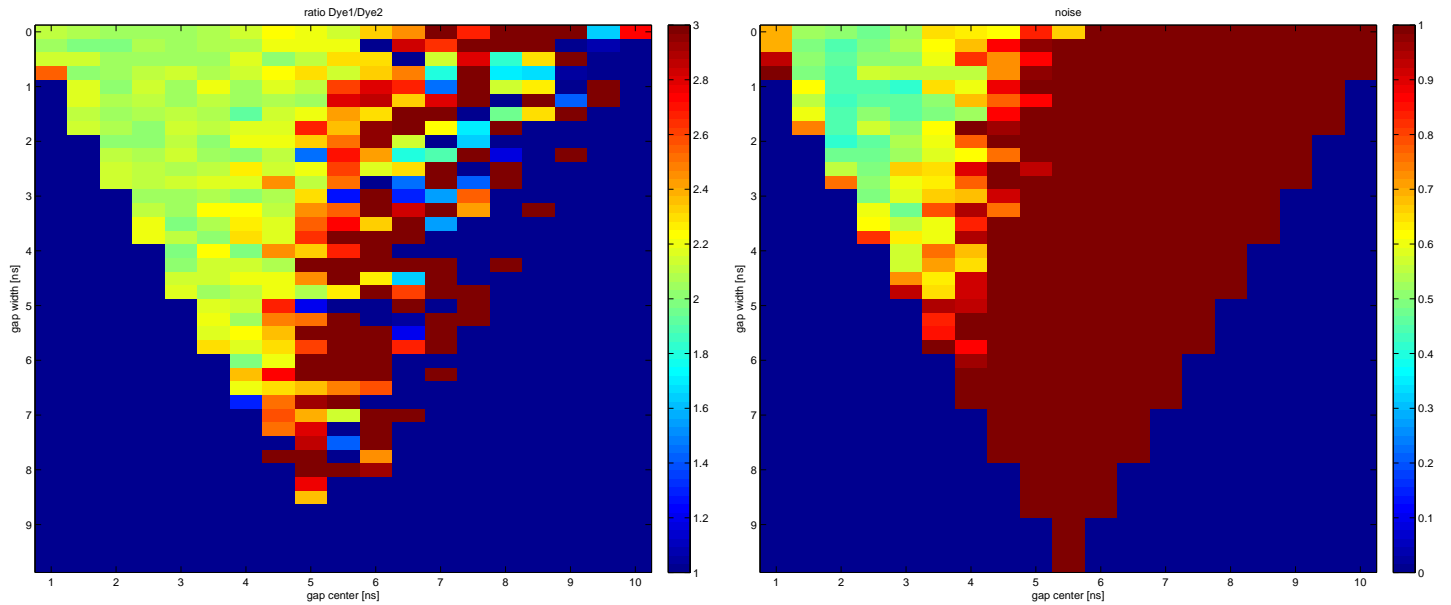
Figure 10: ATTO590 and SiR with lifetimes of 4.08 ns and 3.37 ns and photon counts of 400 and 200.

For the measured lifetimes of ATTO590 and SiR-647 no separation with the used number of photon counts is achievable in my simulation.

c) High Signal

In this simulation the number of photons per dye was set to 1000 for photonsONE and 500 for photonsTWO.

c.1) Hypothetical dyes with well separated lifetimes



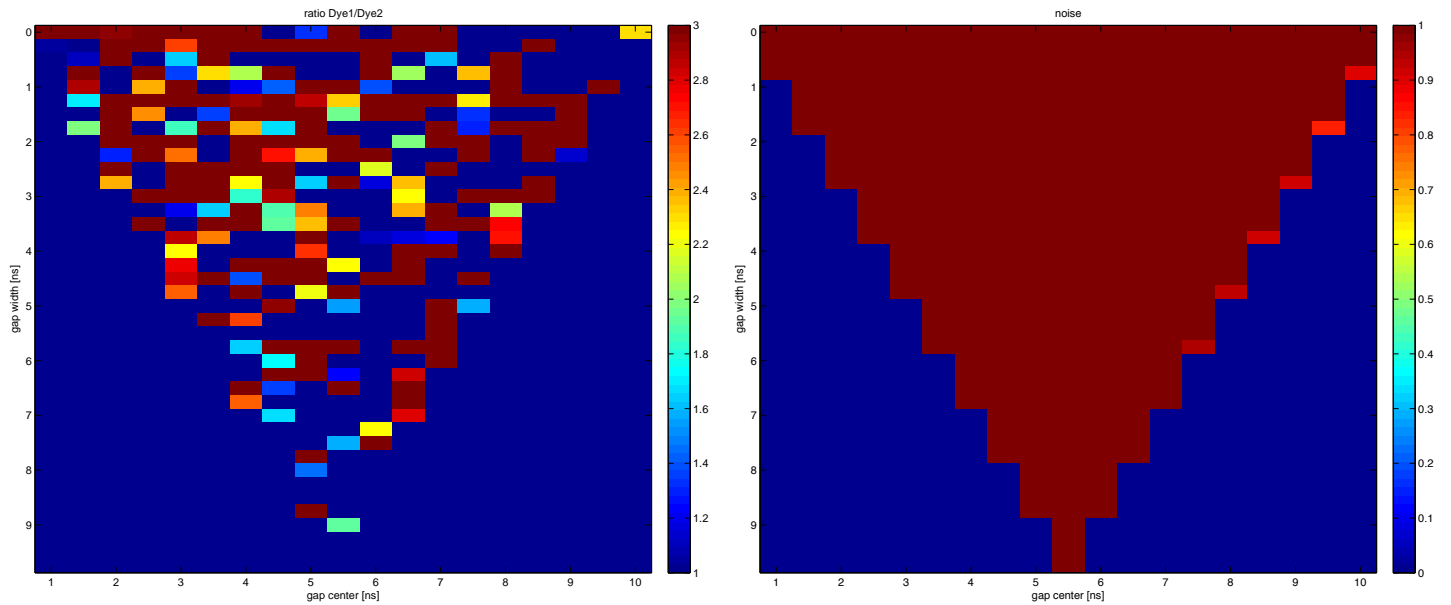
(a) Ratio of Dye1/Dye2

(b) Noise

Figure 11: Hypothetical dyes with lifetimes of 4 ns and 2 ns and photon counts of 1000 and 500.

With these "best case" simulated settings, a lifetime difference of 2 ns and very "high" photon counts, a separation of two different dyes with lifetimes of 4 ns (for the first fluorophore) and 2 ns (for the second fluorophore) is possible. However, the standard deviation of the estimated ratio due to the simulated shot-noise is still about 0.5, corresponding to about 25 % of the resulting signal.

c.2) Lifetime of ATTO590 and SiR-647



(a) Ratio of Dye1/Dye2

(b) Noise

Figure 12: ATTO590 and SiR-647 with lifetimes of 4.08 ns and 3.37 ns and photon counts of 1000 and 500.

The separation of ATTO590 and SiR-647 with my empirically measured lifetimes was not possible in my simulation, even with these "high" photon counts.

To get a good result in our case, the separation of the two dyes has to be about 2 ns and the amount of counted photons has to be extremely high, which we might not get in live time measurements.

My results show that it is challenging to separate two dyes based solely on their fluorescence lifetimes; even with a "good" lifetime separation of 2 ns and "high" photon counts, which are difficult to achieve in live-cell image sequences.

As expected, an increase of photon counts (in the second setting: 400 photons for the first fluorophore and 200 photons for the second fluorophore) improves the likelihood of the photon-ratio-estimate of 2 (see Fig. 9, 10). This might allow a separation of dyes with a lifetime of 4 ns and 2 ns. However, the standard deviation of the estimate is about 0.7, corresponding to an error of more than 36 %. The (light green) area of the photon-ratio-estimate of 2 achieved in my simulation using 400 and 200 photons per dye and my empirically measured lifetimes is smaller compared to the resulting area using lifetimes of 4 ns and 2 ns. Furthermore, due to simulated shot-noise, the standard deviation of the estimated ratio is always higher than 1, corresponding to more than 50 % of the resulting signal. Hence, the program could not separate the two dyes with the given photon counts (400 and 200) and setting for fluorescence lifetime.

In the last setting, using photon counts of 1000 and 500 a separation of dyes with 4 ns and 2 ns lifetimes would be possible (see Fig. 11). Nonetheless, in my hands, separation using my simulation with empirically measured lifetimes of ATTO590 and SiR-647 was not possible. Figure 12 shows that a photon-ratio-estimate of 2 is hardly achieved with these dyes. Moreover, the standard deviation of the ratio estimate is always higher than 1, corresponding to more than 50 % of the resulting signal.

3 Photobleaching

Per definition bleaching is the photochemical alteration of a dye or a fluorophore molecule such that it permanently is unable to fluoresce. This is caused by cleaving of covalent bonds or non-specific reactions between the fluorophore and surrounding molecules.

Photobleaching has a linear dependence on weak excitation light irradiance with one-photon excitation. High excitation irradiance may also introduce nonlinearity even in one-photon excitation.¹⁴

I was interested in the bleaching behavior of the popular SiR-647 dye on our custom-built STED nanoscope. However, I was not able to find a systematic quantification of bleaching for the SiR-647 dye. Therefore, I conducted a preliminary study to quantify the bleaching behavior of the SiR-647 dye. Experiments were run on a custom-built STED nanoscope, so the results presented here may not be reproducible on other setups. My experiments aimed to answer the following questions:

- How does the imaged field of view (FOV) affect the bleaching rate?
- How do different oxygen scavenging buffers affect the bleaching rate?

I conducted experiments in fixed cells as well as living cells. My results are summarized in the next sections.

3.1 Bleaching and the field of view size

To investigate the (subjective) notion that the bleaching rate does not scale linearly with the size of the FOV, I recorded a set of bleaching curves (total fluorescence intensity as a function of time) from cells labeled with SiR-647. Bleaching curves were recorded with different FOV sizes. My results are presented in the following

¹⁴Yong Wu, "Resonant Scanning with Large Field of View Reduces Photobleaching and Enhances Fluorescence Yield in STED Microscopy", *Sci. Rep.* 5, 14766 (2015)

figures, where the recorded "total intensity" is normalized to the initial datapoint and plotted as a function of time (i.e. the number of imaged frames).

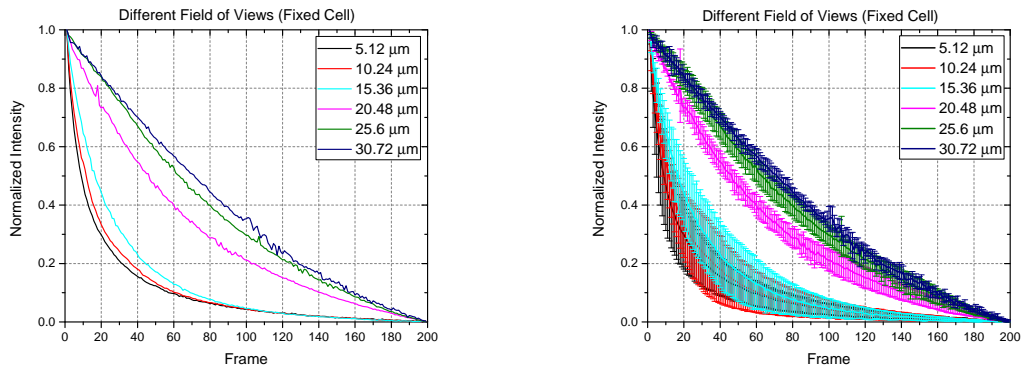


Figure 13: Bleaching curves for different FOVs in fixed cells. Variation of a $5.12 \mu\text{m} \times 5.12 \mu\text{m}$ to a $30.72 \mu\text{m} \times 30.72 \mu\text{m}$ field of view. Each curve represents the average trace from five different cells. Standard deviations are shown in the figure on the right.

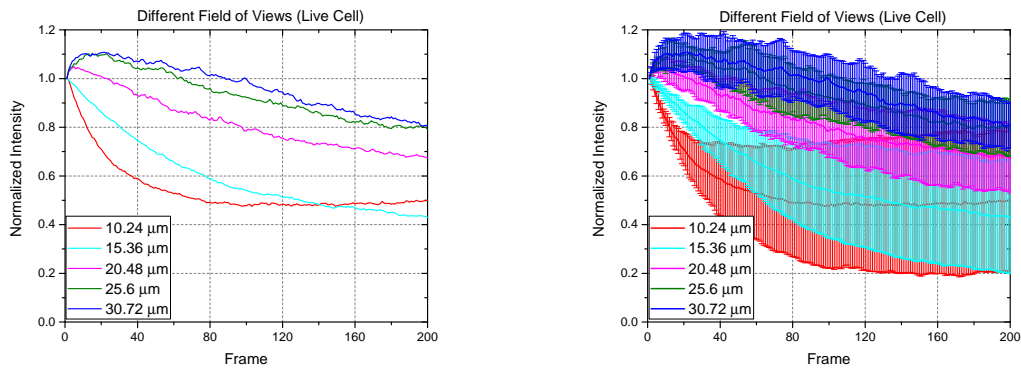


Figure 14: Bleaching curves of SiR dye for different FOV in living cells. Variation of a $5.12 \mu\text{m} \times 5.12 \mu\text{m}$ to a $30.72 \mu\text{m} \times 30.72 \mu\text{m}$ field of view. Each curve represents the average trace from five different cells. The increasing signal intensity at the first frames attributed to motion of labeled structures within the cell. Standard deviations are shown in the figure on the right.

Not surprisingly, a decreasing FOV results in more rapid photobleaching (as each fluorophore is exposed for a longer time). Unfortunately, I was not able to extract

an exact relationship between bleaching rate and FOV size from these data (see Fig. 13 and 14).

3.2 Photobleaching and oxygen scavenging buffers

Different oxygen scavenging buffers may alleviate bleaching by reducing the amount of reactive oxygen in the sample. I conducted bleaching measurements similar to those presented previously, but now varying the medium (i.e. different oxygen scavenging buffers). Bleaching curves were acquired with a FOV of $10.24 \times 10.24 \mu\text{m}$, while the laser powers was held constant (Exc. $50 \mu\text{W}$, Depl. 320 mW) for all measurements.

dStorm Buffer

The dStorm buffer reduces oxygen in the sample. Of course, a reduction of the oxygen level in the sample will also reduce the probability of creating reactive oxygen. However, living cells will suffer, as they need oxygen to survive. To circumvent, this issue normal medium of the cells is replaced with dStorm buffer just before imaging starts. The procedure is described in the appendix B.3.1.

OxyFlour (Oxyrase)

Oxyrase is a commercially available product which claims to reduce the concentration of reactive oxygen in the buffer solution. In contrast to the dStorm buffer, OxyFlour acts only on reactive oxygen and leaves the non-reactive oxygen in the buffer solution, a feature which may make this buffer more suitable for live-cell imaging. As for the dStorm buffer, OxyFlour was introduced to the cells immediately before imaging was commenced. See details in the appendix B.3.2.

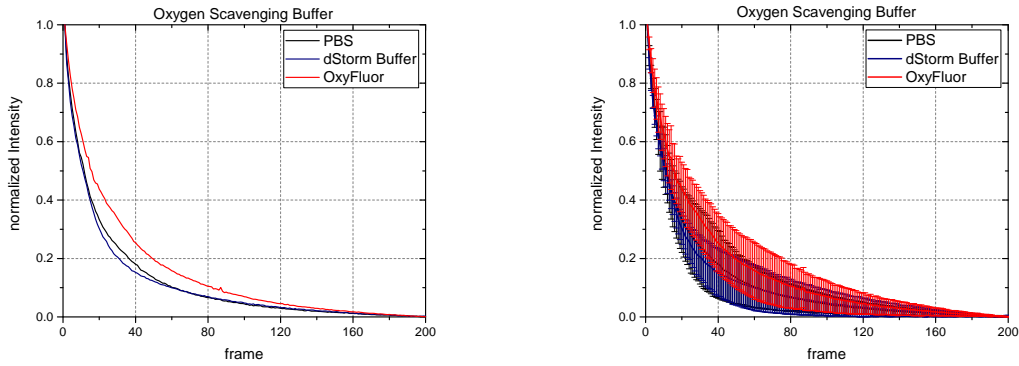


Figure 15: Different buffers in fixed cells. The figure shows bleaching curves of the SiR-647 dye in three different media. Standard deviations are shown in the figure on the right.

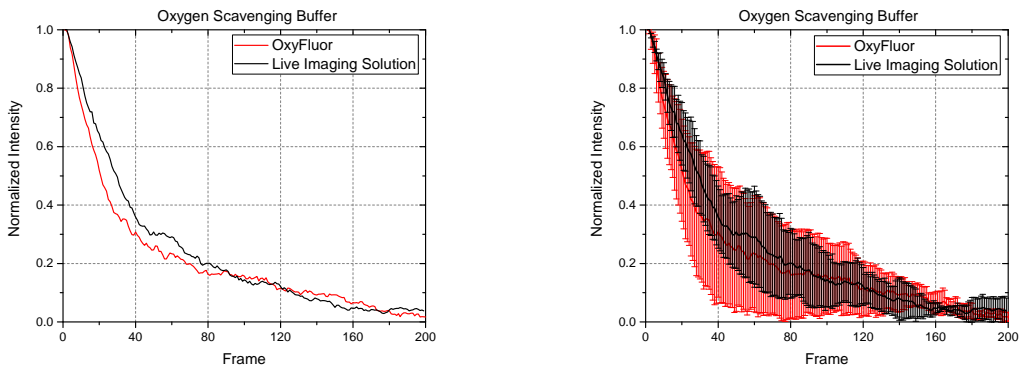


Figure 16: Different buffers in living cells. The figure shows bleaching curves of the SiR-647 dye in OxyFluor and in Live Imaging Solution. Standard deviations are shown in the figure on the right.

Note: We also tried the dStorm buffer for live cell experiments, however, it killed the cells immediately.

3.3 Conclusion on bleaching experiments

My results suggest that bleaching of the SiR-647 dye is lower when increasing the image size (or FOV) for fixed cells as well as for living cells. Unfortunately, I was not able to extract an exact relationship between bleaching rate and FOV size from these data (see Fig. 13 and 14).

Interestingly, as can be seen in Figures 15 and 16, different oxygen scavenging buffers (like OxyFluor and the dStorm buffer) did not have a great impact on the bleaching behavior (when compared to the conventional medium, phosphate-buffered saline (PBS)), in my fixed cell experiments. The bleaching curve of SiR-647 in dStorm buffer is almost the same as the PBS-control-curve (see Fig. 15). There is, however, a slight lowering of the bleaching rate when using OxyFluor solution in fixed cells. Therefore, I can recommend using OxyFluor when imaging fixed cells stained with SiR-647.

Bleaching is primarily a challenge when imaging live-cell dynamics. Given the results from my fixed-cell experiments, it is interesting that my live-cell experiments (see Figure 16) show that the OxyFluor buffer did not improve the bleaching behavior. However, I cannot completely dismiss the usefulness of OxyFluor for live-cell imaging, due to the large standard deviations of the bleaching traces from my live-cell experiment.

A Matlabcode

```
% this is a simulation for getting the diagram of ratio
    between the
% concentration of the dyes and their standard deviation

%% clear everything
clear all; clc

%% input parameters for different dyes

% Parameters for dye ONE
lifeTimeONE = 4;
photonsONE = 50;

% Parameter for dye Two
lifeTimeTWO = 2;
photonsTWO = 25;

%% make the combined lifetime curve
curveLength = 20;
timeStep = 0.01;

time = (0:timeStep:curveLength).';
lifeTimeCurveONE = (photonsONE/(lifeTimeONE*(1 - exp(-
    curveLength/lifeTimeONE))))*exp(-time./lifeTimeONE);
lifeTimeCurveTWO = (photonsTWO/(lifeTimeTWO*(1 - exp(-
    curveLength/lifeTimeTWO))))*exp(-time./lifeTimeTWO);
lifeTimeCurve = lifeTimeCurveONE + lifeTimeCurveTWO;
```

```

% plot of different and combined lifetimecurve
if 1 == 0
    figure(1)
    plot(time,lifeTimeCurve,'k')
    hold on
    plot(time,lifeTimeCurveONE,'b')
    plot(time,lifeTimeCurveTWO,'r')
    hold off
    xlabel('time')
    ylabel('signal')
shg
end

%% Parameters for GAP between two windows
% increasing of gap between detection windows per
iteration
increasingTimeStepGAP = 0.25;

% Parameter for time window ONE
startWindowONE = 0;

% Parameter for time window TWO
endWindowTWO = 20;

%% loop over different starttime Gaps
X = 40; %X=((endWindowTWO-startWindowONE)\2)\0,25 highest
steps of windowwidth between two detection windows
which can get achieved
%M = 19; %M=highest number of the startTimeGAP
%allDividedConcentrations = zeros(X,M);

```

```

% for i = 2:M;
for i = 1:19; % this loop changes the center position for
the gap

    endWindowONE = i;
    startWindowTWO = i;

    %% loop over increasing GAP (=windowwidth)
    % increases the windowwidth creates for each
    windowwidth a unmixing
    % matrix and calculates the belonging standard
    deviations

m = 1; %
while and(startWindowONE < endWindowONE,
    startWindowTWO < endWindowTWO) % this loop changes
the gap width

    concentrationMatrix = [];
    % amount of photons in window ONE
    % amount of photons of Dye 1 in window ONE
    windowONEphotonsONE = exp(-startWindowONE/
        lifeTimeONE) - exp(-endWindowONE/lifeTimeONE);

    % amount of photons of Dye 2 in window ONE
    windowONEphotonsTWO = exp(-startWindowONE/
        lifeTimeTWO) - exp(-endWindowONE/lifeTimeTWO);

    % amount of photons in window TWO
    % amount of photons of Dye 1 in window TWO

```

```

windowTW0photonsONE = exp(-startWindowTWO/
    lifeTimeONE) - exp(-endWindowTWO/lifeTimeONE);

% amount of photons of Dye 2 in window TWO
windowTW0photonsTWO = exp(-startWindowTWO/
    lifeTimeTWO) - exp(-endWindowTWO/lifeTimeTWO);

% determine unmixing matrix - coefficients
    indicates how much a given dye at unit
    concentration contributes to a given detection
    channel
unmixingMatrix = [windowONEphotonsONE,
    windowONEphotonsTWO; windowTW0photonsONE,
    windowTW0photonsTWO];

for n = 1:100; % loop for getting photons in each
    detection window with poisson noise
    % photons/Signal (Dye 1 and Dye 2) in each
    detection window

    % Signal in detection window one
    windowONEphotons = poissrnd(photonsONE*(exp(-
        startWindowONE/lifeTimeONE) - exp(-
        endWindowONE/lifeTimeONE)) + photonsTWO*(
        exp(-startWindowONE/lifeTimeTWO) - exp(-
        endWindowONE/lifeTimeTWO)));

    % Signal in detection window two
    windowTW0photons = poissrnd(photonsONE*(exp(-
        startWindowTWO/lifeTimeONE) - exp(-
        endWindowTWO/lifeTimeONE)) + photonsTWO*(

```

```

        exp(-startWindowTWO/lifeTimeTWO) - exp(-
        endWindowTWO/lifeTimeTWO)));

% solve linear equation for dyes (S =
    unmixingMatrix A) - combine fluorescence
    Signal1 and Signal2 in a Matrix
S = [windowONEphotons;windowTWOphotons];

concentrationMatrix = [concentrationMatrix; (
    linsolve(unmixingMatrix, S)).']; %Matrix,
    where unknown fluorophore concentration
    with noise for n(=1:N) times is stored
% concentrationDye2 = ((windowTWOphotonsONE +
    windowTWOphotonsTWO) - windowTWOphotonsONE
    *(windowONEphotonsONE + windowONEphotonsTWO
    )/windowONEphotonsONE)/(windowTWOphotonsTWO
    -windowTWOphotonsONE*windowONEphotonsTWO/
    windowONEphotonsONE)
% concentrationDye1 = ((windowTWOphotonsONE +
    windowTWOphotonsTWO) - windowTWOphotonsTWO*
    concentrationDye2)/windowTWOphotonsONE
end;

% Concentration Ratio Matrix
concentrationMatrixGapWidth(m,:) = [(m-1)*
    increasingTimeStepGAP, mean(concentrationMatrix
    (:,1)./concentrationMatrix(:,2))]; % gives the
    mean ratio of the concentration for a special
    start point gap and a certain gap width

```

```

distanceMean(m,:) = abs(mean(concentrationMatrix
    (:,1)./concentrationMatrix(:,2))-(photonsONE/
    photonsTWO)); % size of GAP, startGAPValue,
    endGAPValue, distance of value to mean value

% Standard Deviation of Concentration Ratio
standDeviationConcentration(m,:) = std(
    concentrationMatrix(:,1)./concentrationMatrix
    (:,2)); % [ size of GAP, startGAPValue,
    endGAPValue, standard deviation] for this gap
    start and this certain gap width
%standDeviationConcentration(m,:) = std(
    concentrationMatrix(:,1))./std(
    concentrationMatrix(:,2)); % [ size of GAP,
    startGAPValue, endGAPValue, standard deviation]
    for this gap start and this certain gap width

m = m + 1;

endWindowONE = endWindowONE - increasingTimeStepGAP
    ;
startWindowTWO = startWindowTWO +
    increasingTimeStepGAP;
clear concentrationMatrix
end

allConcentrationMatrixGapWidth(1:length(
    concentrationMatrixGapWidth), i) =
    concentrationMatrixGapWidth(:,2);

```



```

allDistanceMean(1:length(distanceMean), i) =
    distanceMean;

allStandDeviationConcentration(1:length(
    standDeviationConcentration),i) =
    standDeviationConcentration;

%% Plots
%figure of fraction over gap width (for one center
    gap)
if 1==0;
    figure
    plot(concentrationMatrixGapWidth(:,1),
        concentrationMatrixGapWidth(:,2),'.')
    axis([0 15 0 5])
    xlabel('GAP widht [ns]')
    ylabel('Ratio of Dye1 and Dye2')
    shg
    set(gcf,'PaperOrientation','landscape');
    set(gcf,'PaperUnits','normalized');
    set(gcf,'PaperPosition',[0 0 1 1]);
    print(gcf, '-dpdf', ['S:\Julia\SimulationFiles
        \PlotFolder\TestFolder\Hallo1\Test031',
        num2str(m), '.pdf']);
end

% figure of standard deviation of concentration (
    for one center
% gap)
if 1==1;
    figure;

```

```

% plot(concentrationMatrixGapWidth(:,1),
        concentrationMatrixGapWidth(:,2),
        standDeviationConcentration(:,4), 'rx')
errorbar(concentrationMatrixGapWidth(:,1),
          concentrationMatrixGapWidth(:,2),
          standDeviationConcentration, 'rx')
axis([0 15 0 6])
xlabel('GAP width [ns]')
ylabel('Ratio of Dye1 and Dye2')
shg

set(gcf, 'PaperOrientation', 'landscape');
set(gcf, 'PaperUnits', 'normalized');
set(gcf, 'PaperPosition', [0 0 1 1]);
print(gcf, '-dpdf', ['S:\Julia\SimulationFiles
                    \Results\NewResults\BadSignal\
                    SirAtto590Lifetime\RatioWNoise\Picture',
                    num2str(i), '.pdf']);
end

close all

% reset Matrix and ajust start and end time of the
    windows
clear concentrationMatrixGapWidth
clear standDeviationConcentration
clear distanceMean
clear smallestStandDev

end

```

```

%% plots
% plot of ratio
figure;
imagesc([1:10],[0:(X-1)].*increasingTimeStepGAP,(
    allConcentrationMatrixGapWidth));
xlabel('gap center [ns]')
ylabel('gap width [ns]')
caxis([1 3])
colorbar
title 'ratio Dye1/Dye2'
shg

set(gcf,'PaperOrientation','landscape');
set(gcf,'PaperUnits','normalized');
set(gcf,'PaperPosition',[0 0 1 1]);
print(gcf, '-dpdf', ['S:\Julia\SimulationFiles\Results\
    NewResults\BadSignal\SirAtto590Lifetime\ratio', num2str
    (4), '.pdf']);

% plot of ratio to distance to mean
figure;
imagesc([1:10],[0:(X-1)].*increasingTimeStepGAP,(
    allDistanceMean));
xlabel('gap center [ns]')
ylabel('gap width [ns]')
caxis([0 1])
colorbar
title 'distance of ration to mean'
shg

```

```

set(gcf,'PaperOrientation','landscape');
set(gcf,'PaperUnits','normalized');
set(gcf,'PaperPosition',[0 0 1 1]);
print(gcf, '-dpdf', ['S:\Julia\SimulationFiles\Results\
    NewResults\BadSignal\SirAtto590Lifetime\distanceToRatio
    ', num2str(5), '.pdf']);

% plot of noise (stand dev)
figure;
imagesc([1:10],[0:(X-1)].*increasingTimeStepGAP,(
    allStandDeviationConcentration));
xlabel('gap center [ns]')
ylabel('gap width [ns]')
caxis([0 1])
colormap jet
colorbar
title 'noise'
shg

set(gcf,'PaperOrientation','landscape');
set(gcf,'PaperUnits','normalized');
set(gcf,'PaperPosition',[0 0 1 1]);
print(gcf, '-dpdf', ['S:\Julia\SimulationFiles\Results\
    NewResults\BadSignal\SirAtto590Lifetime\Noise', num2str
    (6), '.pdf']);

```

B Sample preparation

B.1 Fixed cell

For all measurements COS7 cells were used. The cells were transfected with Sec61 β using Lipofectamine (standard protocol). The fixation and staining of the cells were also done according to standard protocols. Labelling with SiR-647 dye was at a concentration of about 1 μ M.

B.2 Live cell

For the live cell measurements COS7 cells were transfected with Sec61 β as described in the section B.1. One hour before imaging the cells were stained for half an hour with a 5 μ M concentration of SiR-647 dye. Afterwards, the dye was washed out for another 30 min in normal growth media. Immediately before imaging, the media was exchanged with a mixture of live-cell imaging solution and glucose.

B.3 Oxygen scavenging buffers

B.3.1 dStorm buffer

First, a base buffer of 50 mM Tris PH 8.0, 50 mM NaCl and 10 % glucose were made. Then 10 μ l of glucose oxidase and 2 μ l of catalase got added to the 1000 μ l of the premixed base buffer. This mixture was pipetted in the Matek dish directly on the sample before imaging.

B.3.2 OxyFluor

To make the OxyFluor buffer solution, I mixed a 1:100 dilution of the OxyFluor with a 10 mM DL-Lactate in PBS. For live-cell imaging the OxyFluor and DL-Lactate

mixture was diluted in the live-cell imaging buffer.

C Bleaching analysis

C.1 Oxygen scavenging buffers

I wrote a MATLAB script for extracting bleaching curves from image sequences. In this script, the 10 % brightest pixels of each frame were summed. I note that the resulting curves did not vary much, if I used the 10 to 20 % brightest or the 10 % brightest pixels to quantify image brightness. The lowest value of each bleaching curve was subtracted, making each bleaching curve end at zero. The bleaching curves were then normalized to the first datapoint. Finally, curves from five different cells were averaged to yield one trace with standard deviations.

C.2 Field of view

I used the same MATLAB program as above, but I skipped the minimum-subtraction step, as I could not assume that the region of interest was completely bleached (providing a baseline "zero" signal) at the end of the image sequence.